Title	Understanding the stability of Samanea saman trees through tree pulling, analytical calculations and numerical models
Author(s)	Rahardjo, H.; Harnas, F. R.; Indrawan, I. G. B.; Leong, E. C.; Tan, P. Y.; Fong, Y. K.; Ow, L. F.
Citation	Rahardjo, H., Harnas, F.R., Indrawan, I.G.B., Leong, E.C., Tan, P.Y., Fong, Y.K., et al. (2014). Understanding the stability of Samanea saman trees through tree pulling, analytical calculations and numerical models. Urban Forestry & Urban Greening, 13(2), 355-364.
Date	2013
URL	http://hdl.handle.net/10220/19818
Rights	© 2013 Elsevier GmbH. This is the author created version of a work that has been peer reviewed and accepted for publication by Urban Forestry & Urban Greening, Elsevier GmbH. It incorporates referee's comments but changes resulting from the publishing process, such as copyediting, structural formatting, may not be reflected in this document. The published version is available at: [DOI: http:dx.doi.org/10.1016/j.ufug.2013.12.002].

Understanding the stability of Samanea saman trees through tree pulling, analytical calculations and numerical models

Abstract

There have been several cases of tree failure in Singapore. Many studies have shown that soil properties and root architecture of trees are important factors that govern tree stability. Twenty *Samanea saman* trees were planted in different soil media, which were original in-situ soil, top soil, mixture of 50% granite chips and 50% top soil, and mixture of 80% granite chips and 20% top soil. The objectives of this study were to investigate tree overturning processes and also to compare the results of tree pulling tests with results from an analytical calculation and numerical modeling for different soil types. The results showed that stability of the trees were not governed by the shear strength of the soil. Factors that affected tree stability included cross-sectional area of the roots and root plate area. Tree pulling test and numerical modeling results showed that there were two modes of failure which occurred when a tree was overturned. The first mode was the shear failure of soil and the second was a combination of shear failure of soil and root breakage. The maximum overturning force obtained from the tree pulling test was in the same order of magnitude as the maximum overturning forces obtained from the analytical calculation and numerical modeling.

Keywords: Tree stability, soil mixtures, *Samanea saman*, tree pulling test, finite element modeling.

1. Introduction

Trees are an important component of the urban environment and provide numerous advantages to humans. However, tree failure can cause damage to property and infrastructures and may also cause injury or loss of life. There have been several cases of tree failures associated with low soil strength in Singapore. In order to enhance tree stability, methods to improve the engineering properties of soil for developing a better tree root and soil system need to be investigated.

Fine-grained soils have been commonly used as tree growing media. A mixture of fine-grained soil and coarse-grained soil has been used to overcome the challenges associated with urban trees in relation to tree stability (Grabosky and Bassuk, 1995). As compared to a fine-grained soil, the soil mixture has higher shear strength due to an increase in contact pressure between the coarse-grained particles. In addition, the resulting macro pores allow for tree roots to penetrate, down to a maximum depth and this will enhance the stability of the tree and soil system. Rahardjo et al. (2008) found that shear strength of a soil increased significantly after mixing the soil with more than 50% of granite chips.

Previous studies of tree root systems showed that the strength of tree root anchorage is governed by several factors, such as root architecture (Dupuy et al., 2005; Fourcaud et al., 2008), soil physical and analytical properties (Dupuy et al., 2005), depth, shape and

weight of soil root plate (Coutts, 1986), and the location of the rotational axis during overturning (Mickovski and Ennos, 2002, Fourcaud et al., 2008). Root architecture is an important component of tree stability. However, natural biological variability makes it difficult to model the effect of branching and mechanical properties of the root accurately (Mickovski et al., 2007).

Tree pulling tests had been conducted on trees to study the mechanism associated with tree failures (Peltola, 2006). These tests involved pulling the tree sideways until failure or till a pre-determined displacement occurred. The force required to bring about failure was recorded. Tree failure could occur due to either stem failure or the whole tree overturning (Crook and Ennos, 1996). However, tree pulling is costly and destructive. Therefore, the number of tree that can be pulled to study the mechanism of tree failure is often limited. These limitations make modeling through the use of analytical calculations and numerical methods a more feasible option (Dupuy et al., 2007). Several studies such as those conducted by Dupuy et al. (2005), Fourcaud et al. (2008) and Rahardjo et al. (2009) showed that numerical modeling is a very useful tool in studying the behavior of soil-root interaction.

Rahardjo et al. (2009) proposed two failure modes associated with the overturning of a tree: shear failure of soil and root failure. Shear failure of soil (SFS) occurs along a slip surface without having any additional resistance from the roots. Root failure mode occurs when the resistance of the root system in withstanding the load is exceeded. These root

resistances are shear resistance in the transverse plane, slippage resistance and tensile resistance. When the applied force exceeds these resisting forces, there will be three possible modes of root failure: (i) shear failure of root system (SFRS), (ii) slippage of root system (SRS), and (iii) tensile failure of root system (TFRS). Shear failure of root system occurs if the shear stresses imposed to the roots are higher than the shear strength of the roots. Slippage of root system occurs when the slippage force exceeds the adhesion between the root and the soil. Tensile failure occurs when the tensile stress acting on the roots exceeds the tensile strength of the roots. The forces involved in the analytical calculation are illustrated in Figure 1.

Samanea saman or commonly known as rain tree is easily recognized by its characteristic umbrella-shaped canopy. The tree usually reaches 15 to 25 m in height with a canopy diameter often being wider than the height of the tree. This species is commonly found along the streets, car parks and open park lands in Singapore. *Samanea saman* was used in this study because it tends to develop a shallow root plate in the urban landscape and possesses a high growth rate as compared to other tree species. It is well known that a plate root possesses the least effective resistance to withstand wind load as compared to other types of root architecture such as heart and tap root (e.g. Coutts, 1983).

The objective of this study was to investigate the overturning processes and also to study the results obtained from the tree pulling test which was subsequently compared with the results generated from analytical calculations and numerical models for the different soil

types. For this purpose, pulling/overturning experiments involving twenty trees grown in four different soil mixtures were carried out in the field. The data obtained from the tree pulling tests were then numerically modeled and analyzed using analytical calculations and a numerical method.

2. Material and Methods

2.1 Study site and soil engineering properties

The experiment was conducted on an open land in the western end of Singapore. A total of 20 rain trees had been planted for three years in a tree pit of 2.5 m x 2.5 m and 1.0 m depth. The ages of the trees when planted were approximately three years old with heights of around three meters. There were four soil mixtures used in the experiment namely top soil (TIF), original in-situ soil (IIF), 50% Granite chips and 50% Top Soil (50GC-50TS) and 80% Granite chips and 20% Top Soil (80GC-20TS). Details of the soil mixtures are given in Rahardjo et al. (2008). There were five trees planted in each soil mixture. The trees were planted in a random arrangement as illustrated in Figure 2.

TIF used in this research was brown in color and consisted of loamy soil, organic matter (compost), and sand on a volume basis ratio of 3:2:1, respectively. Percentages of granite chips used in the mixture for improving the soil shear strength in this study were 50% and 80% on dry mass basis. To compare the performance of soil improvement, trees were also planted in the original in-situ soil (IIF). Soil testing was conducted in accordance with ASTM standards. Soil moisture content was determined by drying soil samples at a

predetermined temperature in accordance with ASTM D-2216 (1998), while the field density test was conducted following the sand replacement method using sand cone apparatus in accordance with ASTM D-1556 (2003). The particle size determination was conducted using a sieve analyses in accordance with ASTM D-422 (1998). Shear strength measurement for the TIF (top soil) and IIF (original in-situ soil) was carried out using consolidated-undrained triaxial tests with pore pressure measurement in accordance with ASTM D-4767 (1995). The shear strength data for the 50GC-50TS and 80GC-20TS were already reported in Rahardjo et al. (2008). The shear strength of a soil can be represented by the Mohr-Coulomb failure criterion as follows:

$$\tau_{ff} = c' + \left(\sigma_f - u_w\right)_f \tan\phi' \quad (1)$$

where τ_{ff} is the shear stress on the failure plane at failure (kPa), *c'* is the effective cohesion, which is the shear strength intercept when the effective normal stress is equal to zero, (kPa). $\left(\sigma_f - u_w\right)_f$ is the effective normal stress on the failure plane at failure (kPa), σ_{ff} is the total normal stress on the failure plane at failure (kPa), u_{wf} is the pore-water pressure at failure (kPa) and ϕ' is the effective angle of internal friction (^{o}). The grain size distributions of the soil mixtures used in this study are shown in Figure 2. The mixing of granite chips and top soil resulted in a very compact soil structure that had a high shear strength as shown in the summary of soil engineering properties presented in Table 1.

2.2 Tree pulling test

Before conducting the tree pulling test, several tree characteristics such as girth circumference, tree height, stem volume and crown width were recorded. The tree pulling test was conducted using an automated winch (Ingersoll Rand-FA7) which was capable of providing a maximum load of seven (7) metric tonnes. When the tree was pulled sideways, the crown has a higher lateral displacement as compared to the stem of the tree. Therefore, the crown can exert additional overturning moment to the root system. This additional moment is a function of the crown volume. The trees in the tree pulling test had different crown volumes. Therefore, the crowns of the trees were pruned to remove all lateral branches in order reduce the effect of crown weight on the overturning force during the tree pulling test. The winch was positioned on a fix platform that had been customized to the general height of the trees and an attachment was placed on the tree at a height of 1.3 m from the ground . The winch was then connected to a dynamometer (Dillon Edxtreme-Edx-2T) by a sling which was capable of recording forces up to 200 kN and then connected to the tree. The dynamometer was connected to a wireless device that transmitted the data to a personal computer. A distometer was used to measure the deflection of the tree and it was positioned at the opposite side of the winch. A high resolution digital camera and a video camera were used to record the overturning process. The tree was pulled at a constant rate of 6 cm per second. The resistance force and the corresponding displacement were measured in intervals of one second. The test was terminated when the force registered was constant or declined from the peak force. After failure, the root-soil plate depth and diameter of the slip surface were measured and recorded. The set-up of the tree pulling test

153 is presented in Figure 3. After conducting the tree pulling test, the soil and the roots were
154 air-spaded and the tree was removed for further measurements. The total cross-sectional
155 area of the roots (CSA) was measured following a technique proposed by Nicoll and Ray
156 (1996). The diameter of each lateral root larger than 1 cm was recorded at 50 cm distance
157 from the centre of the tree and the CSA was calculated using the following equation:
158

159 $$CSA = \pi\left(\frac{d_h + d_v}{4}\right)^2 \quad (2)$$

160

161 where d_h is the horizontal diameter of the roots and d_v is the vertical diameter of the roots.

162

163 One-way analysis of variance (ANOVA) is a statistical method that is commonly used to
164 compare more than two population means. One-way ANOVA was performed using SPSS
165 software to investigate the effect of different soil conditions on the measured tree
166 characteristics and the effect of different soil conditions on the pulling force. The null
167 hypothesis was that the means of each dependant variables were equal or there was no
168 significant difference in the variables. An α value of 0.05 was used in the one-way ANOVA
169 statistical analyses.

170

171

172

2.3 Analytical calculation

Analytical calculation was performed to determine the forces required to overturn the tree. There were two steps involved in the analytical calculation. The first step was to analyze the resisting shear force generated by the soil using the ordinary method of slices (Fellenius, 1936) that is commonly used for slope stability analysis. Root-soil plate depth and diameter of the slip surface were determined based on the pulling test measurements. The second step was to analyze the resistance of the root system as suggested by Rahardjo et al. (2009) using the following equations. In this study, the shear strength of the wood was assumed to be 0.5 MPa and the tensile strength of the root was assumed as 4.3 MPa (Ziemer, 1978).

The resisting shear force (F_{shear}) provided by the roots is determined as:

$$F_{shear} = \sum_{i=1}^{N} A\tau_{shear} \quad (3)$$

where N is the number of roots, A is the surface area of the root (m^2) and τ_{shear} is the shear strength of root (kPa)

The resisting slippage force (F_{slip}) provided by the roots is expressed as:

$$F_{slip} = \sum_{i=1}^{N} KL_{slip}\tau_{slip} \quad (4)$$

where N is the number of roots, K is the circumference of each root (m), τ_{slip} is the slippage strength between soil and root and L_{slip} is the length of horizontal root providing the slippage resistance.

The resisting tensile force ($F_{tensile}$) provided by the roots is calculated as follows:

$$F_{tensile} = \sum_{i=1}^{N} A\tau_{tensile} \quad (5)$$

where $\tau_{tensile}$ is the tensile strength of root (kPa)

2.4. Numerical Modeling

The numerical modeling of tree stability during the pull out test was performed using SIGMA/W (Geo-Slope International Ltd) software. The problem was modeled as a plane strain, two-dimensional stress-strain finite element model as shown in Figure 4. The model consisted of three main parts. The first part was the surrounding in-situ soil of 20 m width and 8 m depth. The second part was the soil inside the tree pit of 2.5 m width and 2.0 m depth. The third part was the root model using the diameter taken as an equivalent diameter calculated from the sum of individual root cross section area (CSA) measured at 50 cm from the stem of the tree. The last part was the stem whose dimensions were also obtained from the field measurement. The finite element mesh of the model consisted of triangular elements. The adhesion between soil and root was ignored in the numerical

modeling. The boundary conditions of the surrounding soil were taken as zero horizontal displacement on both vertical sides and zero displacement in both directions at the bottom of the model as shown in Figure 4.

For the numerical modeling, the soil was modeled as an elastic-perfectly plastic material. The elastic part was governed by the modulus of elasticity (E) and Poisson's ratio (ν) of the soil. The modulus of elasticity of the soil was taken from the initial tangent of stress-strain curve as obtained from the shear strength test on a saturated soil sample. The yield point was defined in accordance with the Mohr-Coulomb failure criterion. If the stress exceeds the yield point, the stress-strain curve will be a horizontal line, representing the plastic condition of soil. Root material was considered as an elastic-perfectly plastic material with a modulus of elasticity of 5×10^6 kPa and a Poisson's ratio of 0.3 and a maximum yield stress of 10^3 kPa (Carmichael, 1984).

An incremental force of 0.1 kN was applied in 100 time steps on the tree stem at 1.3 m from the ground surface. Displacement, shear stress and strain were computed at every time step. The force-displacement curve was generated to represent the behavior of the tree-root system by plotting the incremental force against the displacement at the point where the force was applied.

3. Results

3.1. Tree pulling test results

Trees planted at the study site were six years old at the time of the pull-out tests. The average height and girth circumference of the trees were 6.58 ± 0.25 m and 50.6 ± 8.6 cm, respectively. The average crown diameter of the trees was 6.2 ± 1.9 m. Statistical analyses using one-way ANOVA test showed that the average height and diameter, and the crown diameter were not affected by different soil conditions as shown by the summary on tree characteristics detailed in Table 2.

As the tree overturned, the soil in the windward side of the tree experienced tension, whereas the soil in the leeward side of the tree experienced compression. Two typical force-displacement curves from the tree pulling test are shown in Figure 5. The failure force was defined as the force at which the tree started to experience excessive stem displacements without any increase in the measured force. The failure force was reached when the root strength was exceeded or the soil-root plate overturned. Curve for Tree#19 (Figure 5) represents a tree with root failure and curve Tree#3 represents a tree with soil plate overturning or soil failure. The force-displacement curve of root failure showed a high overturning force that could be sustained for some time after root failure had occurred and until the tree was completely overturned. The force-displacement curve of soil usually showed a low overturning force that dropped suddenly when soil failure occurred.

253 Results of one-way ANOVA for the maximum pulling force required to uproot the trees
254 planted in different soils are also summarized in Table 2. While a significant difference was
255 not identified (p=0.493), it was shown that trees planted in IIF (original in-situ soil) had the
256 highest mean maximum pulling force, while the trees planted in 50GC-50TS had the lowest
257 mean maximum pulling force.
258
259 The maximum overturning force required to overturn each tree in the tree pulling test is
260 summarized in Appendix 1 along with the different soil types, cross-sectional area of the
261 root, root plate depth and root plate radius. The highest maximum overturning force
262 occurred in Tree#19 planted in IIF (original in-situ soil) with a maximum overturning force
263 of 20.8 kN while the lowest maximum overturning force occurred in Tree#17 planted in
264 80GC-20TS soil with a maximum overturning force of 0.6 kN. There were variations in the
265 maximum overturning force for trees planted in the same soil. These variations showed that
266 the maximum overturning force was not dependent on the soil type. Figure 6a and Figure
267 6b shows the relationship between maximum overturning forces for the trees planted in IIF,
268 TIF, 50GC-50TS, and 80GC-20TS against root plate radius and cross-sectional area and
269 root plate depth, respectively. There were relatively strong relationships between the
270 maximum overturning force and root plate radius (R^2=0.56) and also between the
271 maximum overturning force and root cross-sectional area (R^2=0.61) as compared to the
272 relationship between the maximum overturning force and the root plate depth (R^2=0.21).
273
274

3.2. Analytical calculation

The input data for analytical calculations were taken from the tree pulling test. The formulas used were similar to the formulas used by Rahardjo et al. (2009) and are presented in Section 2.4 of this paper. The results of the analytical modeling for different failure modes are shown in Figure 7. The results show that the highest maximum overturning force to overturn a tree is associated with the tensile failure of the root system (TFRS), while the lowest maximum overturning force to overturn a tree is associated with the slippage of root system (SRS). The highest maximum overturning force occurred in Tree#20 planted in 80GC-20TS soil for all failure modes, whereas the lowest maximum overturning force occurred in Tree#17 planted in 80GC-20TS for SFRS and TFRS failure modes and Tree#18 planted in TIF for SRS and SFS failure modes. Tree#20 has the highest maximum overturning force due to its high CSA and its widest radius of root plate among the other trees. Tree#17 has the lowest CSA among all trees which resulted in a lower shear and tensile capacity of the roots. However, the root plate of Tree#17 was deeper than the root plate of Tree#18 which resulted in a higher soil shear and root slippage resistance for Tree#17.

3.3. Numerical modeling

The force-displacement curves obtained from the numerical modeling show two typical patterns as shown in Figure 8a. The first pattern with a lower overturning force at failure represents a typical curve for the mode of shear failure of soil (SFS). The SFS failure mode occurred when the root length was shorter than the radius of the slip surface of soil. The

297 second pattern with a higher failure force represents a typical curve for a combination of
298 SFS and shear failure of root system (SFRS) which usually occurred in trees with roots that
299 intersected the slip surface of soil. An illustration of these failure modes is shown in Figure
300 8b and Figure 8c. The SFS failure mode usually developed at the edges of the root zone,
301 whereas the combination of SFS and SFRS usually developed at the root zone resulting in
302 almost a similar size of the failure root plate. The maximum forces required to overturn the
303 trees and the failure modes obtained from the numerical modeling are presented in Figure
304 9. The failure modes obtained from the numerical modeling (SFS and combination of SFS
305 and SFRS) were generally similar to the failure modes obtained from the tree pulling tests
306 (soil failure and combination of soil failure and root breaking). The highest maximum
307 overturning force observed in the numerical modeling was associated with Tree#20 which
308 was similar to the analytical calculation result whereas the field tree pulling tests showed
309 that Tree#19 has the highest maximum overturning force. The lowest maximum
310 overturning force observed in the numerical modeling was associated with Tree#3 whereas
311 the analytical calculation and the field tree pulling tests showed that Tree#17 has the lowest
312 maximum overturning force.
313
314 For SFS failure mode, the numerical modeling and analytical calculation over-predict the
315 maximum overturning forces obtained from the field overturning experiment as shown in
316 Figure 10a. For the combination of SFS and SFRS failure mode, the maximum overturning
317 forces obtained from the numerical modeling were in the same order as compared to the
318 maximum overturning forces obtained from the tree pulling test whereas the maximum

319 overturning forces from the analytical calculation over-predicted the maximum overturning
320 forces obtained from the field overturning experiment as shown in Figure 10b.
321
322 **4. Discussion**
323 Mixing top soil with granite chips increased the shear strength parameters of the soil
324 (Rahardjo et al., 2008). However, the increased shear strength of the soil did not guarantee
325 a larger resistance to overturning for trees as shown in the field test results. This was
326 shown by the results of the statistical analysis of overturning forces for different soil
327 conditions. The statistical analyses showed that the difference in the mean overturning
328 force was statistically insignificant. The statistical analyses in tree characteristics for
329 different soil conditions also showed that the difference in mean tree characteristics was
330 statistically insignificant. The statistically insignificant difference in the tree characteristics
331 planted in different soil conditions may have led to the statistically insignificant difference
332 in the overturning force for trees planted in different soil conditions.
333
334 Although, it was found that different soil conditions yielded a statistically insignificant
335 difference in the overturning force, the tree pulling test result showed that there were linear
336 relationships between root cross-sectional area (CSA) and root plate radius with the forces
337 needed to overturn the tree. This was similar to reports by Nicoll and Duncan (1996),
338 Crook and Ennos (1998) and Mickovski and Ennos (2002). This shows that the root
339 properties such as the root cross-section area (CSA) and root plate radius were in fact very
340 crucial in tree stability. In addition, the root CSA and root plate radius values were not

affected by the soil medium as shown by the statistical analysis. Therefore, further studies on methods to increase root CSA and root plate radius are necessary in order to enhance our understanding of tree stability. It was also found that the root plate depth did not greatly affect the maximum overturning force of *Samanea saman* unlike the results found by Moore (2000) on *Pinus Radiata* or Abd. Ghani et al. (2009) on *Eugenia grandis*. This might be caused by the fact that the depth of the root plate in *Samanea saman* was generally shallow as compared to the depth of root plate in these other species. Thus, the limited range of root plate depth created a statistically insignificant difference in the overturning force.

Based on soil shear strength tests results, IIF (original in-situ soil) was one of the weakest soils; however, the highest maximum overturning force recorded from the tree pulling test was the force required to overturn Tree #19 that was planted in IIF soil. The force required to overturn Tree#19 was higher than the force required to overturn Tree #20 which was considered to have the highest overturning force based on the analytical calculation and numerical modeling. Several factors might have contributed to this difference such as the root orientation and the variation of the root strength in the field. The effect of root orientation and clustering might affect the maximum overturning force as suggested by Abd. Ghani et al. (2009). The roots that were found in the windward direction of a tree with a plate root tended to have a higher overturning force as reported by Ennos (2000). The shear and tensile strengths of the root vary between tree to tree and also vary for the same tree as it moves further away from the tree's stem as suggested by Bischetti et al. (2005) and Genet et al. (2008).

Field overturning experiments showed that there were two governing failure modes which were visually determined by the condition of the roots. If the root was not broken, the failure mode would be attributed to the shear failure of the soil (SFS). The second failure mode was associated with root breakage. However, the mechanism of root failure is unknown (i.e shear failure or tensile failure). The numerical modeling performed in this study suggested that two failure modes could have occurred during the field overturning/pulling experiment, These were shear failure of soil (SFS) and a combination of shear failure of soil (SFS) and shear failure of root (SFRS). The maximum overturning forces obtained from the numerical model were comparable to those obtained from the field overturning/pulling experiment. As a result, root breakage observed in the tree pulling test could be attributed to the shear failure of roots (SFRS) as simulated in the numerical model.

In general, the maximum overturning forces obtained from the numerical model overestimated the maximum overturning forces measured in the tree pulling test up to between 15 to 25%. This may have been the result of the variability of shear strength parameters and root properties that was not accounted for in the finite element modeling. The shear strength parameters in the finite element model were obtained from laboratory shear strength tests. The shear strength near the ground surface might vary significantly due to the development of roots during the period of tree growth (Tengbeh, 1993). The root properties might also not be uniform for the entire tree root system (Stokes and Mattheck, 1996). The model also assumes that the root diameter is constant to be equal to

387 the equivalent CSA of the roots. This assumption may have a weakness because the root
388 diameter can be highly variable compared to the root diameter at 50 cm from the trunk
389 used for the CSA calculations. However, similar trends on the factors affecting the
390 maximum overturning force were observed in the numerical model as in the tree pulling
391 test as shown in Figure 11a and Figure 11b.
392
393 The analytical calculation results overestimated the maximum overturning forces for the
394 combination between SFS and SFRS modes. This could be due to the fact that the
395 assumption that all roots failed at the same time when the maximum overturning force
396 reached the failure force might not be the actual case. In reality, failure might have
397 occurred progressively (O'Sullivan and Ritchie, 1993). The selection of values of
398 parameters used in the analytical calculation especially for tensile and shear strength
399 parameters of root was critical because it could greatly affect the maximum overturning
400 force calculation using the analytical solutions and should be investigated further in order
401 to enhance the accuracy of the results obtained.
402
403 The analytical calculation and numerical modeling used in this study required the cross-
404 sectional area of the roots and the root plate depth. These parameters are not easily
405 obtained without an invasive method. Therefore, further improvements of the analytical
406 calculation and numerical models for the prediction of tree stability are required so that
407 these models can eventually have the ability to effectively predict the stability of tree.
408

The study reported in this paper was conducted on twenty trees of one species of the same age. This condition limited the study to one root type which was a plate root. Plate root is the weakest root architecture in withstanding overturning (Coutts, 1983) and therefore, it represented the most critical root architecture for tree stability. Oliver and Mayhead (1974) reported that the wind speed that uprooted trees were actually lower than the measured forces used in the tree pulling test. This might be due to the nature of wind loading that was a continuous and dynamic loading for a long period of time, whereas the field tree pulling test experiment was a static and quick loading test. Therefore, it is appropriate to consider a variety of species, other root architectures and dynamic loading in future studies of similar nature.

5. Conclusions

Shear strength of soil increased when it was mixed with granite chips. However, the increase in soil shear strength alone may not increase the stability of the tree because many factors come into play when considering tree stability. Cross-sectional area of the root and the root plate area were found to be parameters that increase the stability of the tree as observed in the field experiment and numerical analyses. Shear failure of soil and a combination of soil shear failure and root breakage were found to be the prevalent failure modes during tree overturning. The maximum overturning force to reach failure as measured in the field experiment was of the same order of magnitude as the maximum overturning forces obtained from the numerical modeling and analytical calculation.

Acknowledgement

This research was conducted in collaboration between Nanyang Technological University and National Parks Boards Singapore. The authors wish to thank Mr. Andhika Sahadewa and other colleagues for their assistance during the tree pulling test.

References

Abd. Ghani, M., Stokes, A., Fourcaud, T., 2009. The effect of root architecture and root loss through trenching on the anchorage of tropical urban trees (*Eugenia grandis wright*). Trees-Structure and Function 23, 197-209

ASTM, D-2216, 1998. Standard Test Method for Laboratory Determination of Water (Moisture) Content of Soil and Rock by Mass.

ASTM, D-1556, 2003. Standard Test Method for Density and Unit Weight of Soil in Place by the Sand-Cone Method.

ASTM, D-422, 1998. Standard Test Method for Particle-Size Analysis of Soils.

ASTM, D-4767, 1995. Consolidated Undrained Triaxial Test for Cohesive Soils.

Bischetti, G.B., Chiaradia, E.A., Simonato, T., Speziali, B., Vitali, B., Vullo, P., Zocco, A., 2005. Root strength and root area ratio of forest species in Lombardy (Northern Italy). Plant and Soil 278, 11-22

Carmichael, E.M., 1984. Timber Engineering Practical Design Studies. E&F. N. Spon, London.

Coutts, M.P., 1983. Root architecture and tree stability. Plant and Soil 71, 171-188.

Coutts, M.P., 1986. Components of tree stability in Sitka spruce on peaty gley soil. Forestry 59, 173-197.

Crook, M.J., Ennos, A.R., 1996. The anchorage mechanics of deep rooted larch Larix europea x japonica. Journal of Experimental Botany 47, 1509-1517.

Crook, M.J., Ennos, A.R., 1998. The increase in anchorage with tree size of the tropical tap rooted tree *Mallotus wrayi,* King (Euphorbiaceae). Annals of Botany 82, 291-296.

Dupuy, L., Fourcaud, T., Stokes, A., 2005. A numerical investigation into the influence of soil type and root architecture on tree anchorage. Plant and Soil 278, 119-134.

Dupuy, L., Fourcaud, T., Lac, P., Stokes, A., 2007. A generic 3D finite element model of tree anchorage integrating soil mechanics and real root system architecture. American Journal of Botany 94, 1506-1514.

Ennos, A.R., 2000. The mechanics of root anchorage. Advance botanical research 33, 133-157.

Fellenius, W., 1936. Calculation of the Stability of Earth Dams. In: Transaction of the Second Congress on Large Dams, Washington, D.C., Vol. 4. United States Government Printing Office, Washington D.C., pp. 445-463.

Fourcaud, T., Ji J-N., Zhang, Z. Q., Stokes, A., 2008. Understanding the impact of root morphology on overturning mechanism: A modeling approach. Annals of Botany 101, 1267-1280.

471 Genet, M., Kokutse, N., Stokes, A., Fourcaud, T., Cai, X.H., J-N, J., 2008. Root
472 reinforcement in plantations of cryptomeria japonica D. Don: effect of tree age and
473 stand structure on slope stability. Forest Ecology and Management 256, 1517-1572.

474 Grabosky, J. & Bassuk, N., 1995. A new urban tree soil to safely increase rooting volumes
475 under sidewalks. Journal of Arboriculture 21, 187-201.

476 Holtz, R.D., & Kovacs, W.D., 1981. An introduction to geotechnical engineering, Prentice
477 Hall Inc, New Jersey USA, pp. 719.

478 Mickovski, S.B., Bengough, A.G., Bransby, M.F., Davies, M.C.R., Hallet, P.D.,
479 Sonnenberg, R., 2007. Material stiffness, branching pattern and soil matric potential
480 affect the pullout resistance of model root systems. European Journal of Soil Science
481 58, 1471-1481.

482 Mickovski, S.B. & Ennos, A.R., 2002. A morphological and mechanical study of the root
483 systems of suppressed crown Scots pine Pinus sylvetris. Trees - Structure and Function
484 16, 274-280.

485 Moore, J.R., 2000. Differences in maximum resistive bending moments of *Pinus radiata*
486 trees grown on a range of soil types. Forest Ecology and Management 135, 63-71.

487 Nicoll, B.C & Duncan, R., 1996. Adaptive growth of tree root systems in response to wind
488 action and site conditions. Tree Physiology 16, 891-898.

489 O'Sullivan, M.F & Ritchie, R.M., 1993. Tree stability in relation to cyclic loading.
490 Forestry 66, 69-82.

491 Oliver, H.R., & Mayhead, G.J., 1974. Wind measurements in a pine forest during a
492 destructive gale. Forestry 47, 185-194.

493 Peltola, H.M., 2006. Mechanical stability of tree under static loads. American Journal of
494 Botany 93, 1501-1511.

495 Rahardjo, H, Harnas, F.R., Leong, E.C., Tan, P.Y., Fong, Y.K., Sim, E.K., 2009, Tree
496 stability in improved soil to withstand wind loading. Urban Forestry and Urban
497 Greening 8, 237-247.

498 Rahardjo, H, Indrawan, I.G.B., Leong, E.C., Yong, W.K., 2008. Effects of coarse-grained
499 materials on hydraulic properties and shear strength of soil. Journal of Engineering
500 Geology 101, 165-173.

501 Stokes, A., & Mattheck, C., 1996. Variation of wood strength in roots of forest trees.
502 Journal of Experimental Botany 47, 693-699.

503 Tengbeh, G.T., 1993. Effect of grass roots on shear strength variations with moisture
504 content. Soil Technology 6, 287-295.

505 Ziemer, R.R., 1978. An apparatus to measure the cross cut shearing strength of roots.
506 Canadian Journal of Forest Research 8, 142-144.

LIST OF TABLES

TABLES

Table 1 Soil engineering properties

Soil type/ (USCS classification symbol)	Effective cohesion c' (kPa)	Effective angle of internal friction ϕ ' (˚)
TIF (SC)	2	25
IIF (CL)	5	24
50GC-50TS (SC)	5	44
80GC-20TS (GP)	25	48

Table 2. Summary of statistical analyses result of tree characteristic for different soil condition

Characteristic/Soil	IIF	TIF	50GC-50TS	80GC-20TS	P values
Height (m)	6.58±0.15 a	6.50±0.10 a	6.60±0.14 a	6.62±0.15 a	0.932
Girth circumference (m)	0.46±0.01 a	0.50±0.01 a	0.51±0.02 a	0.56±0.01 a	0.424
Crown width (m)	5.57±0.24 a	6.10±1.15 a	6.81±1.34 a	6.47±0.56 a	0.811
Overturning force (kN)	12.19±2.66 a	7.96±1.18 a	6.98±2.74 a	9.85±3.53 a	0.493
Root depth (m)	0.93±0.07 a	1.05±0.2 a	0.68±0.13 a	0.75±0.08 a	0.218
Cross sectional area (CSA) (cm^2)	179.17±49.23 a	118.97±40.16 a	111±37.27 a	231.86±120.29 a	0.598

Mean±standard error. Pairs of values in a column followed by the same letter are not significantly different at the α=0.05 level.

LIST OF FIGURES

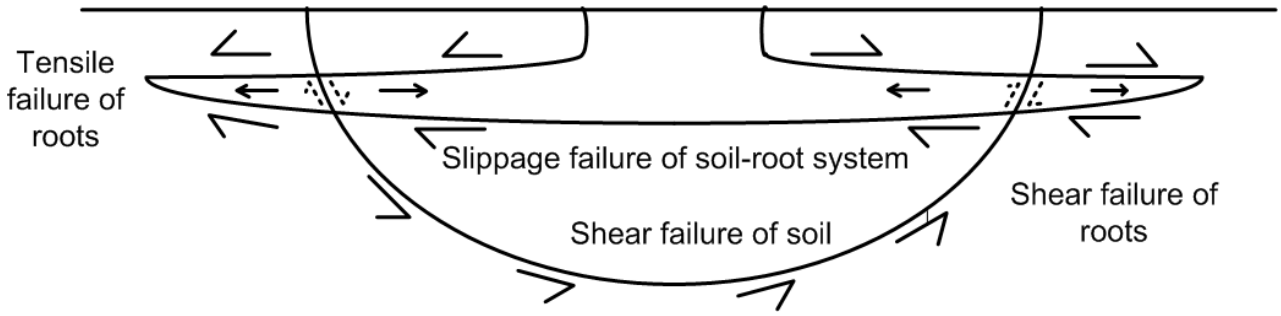

Figure 12 Soil-root interactions (from Rahardjo et al., 2009)

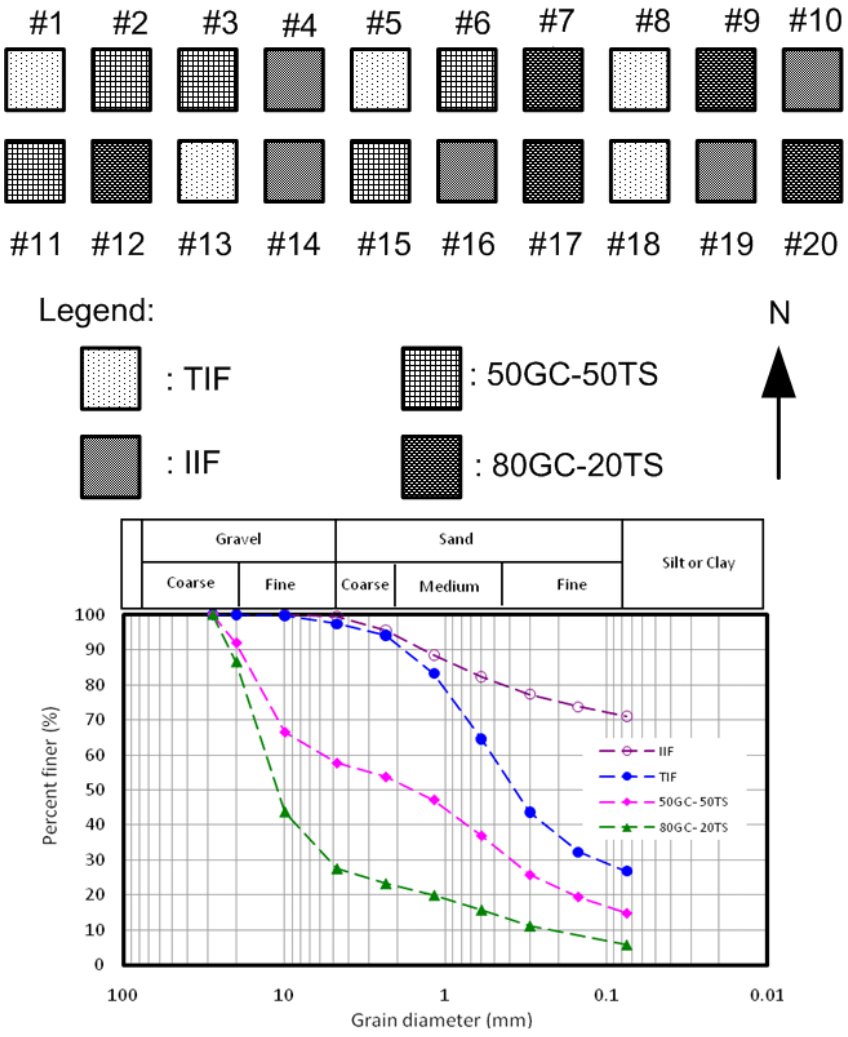

Figure 13 Soil type arrangement for tree planting and grain size distributions of soils used in the study

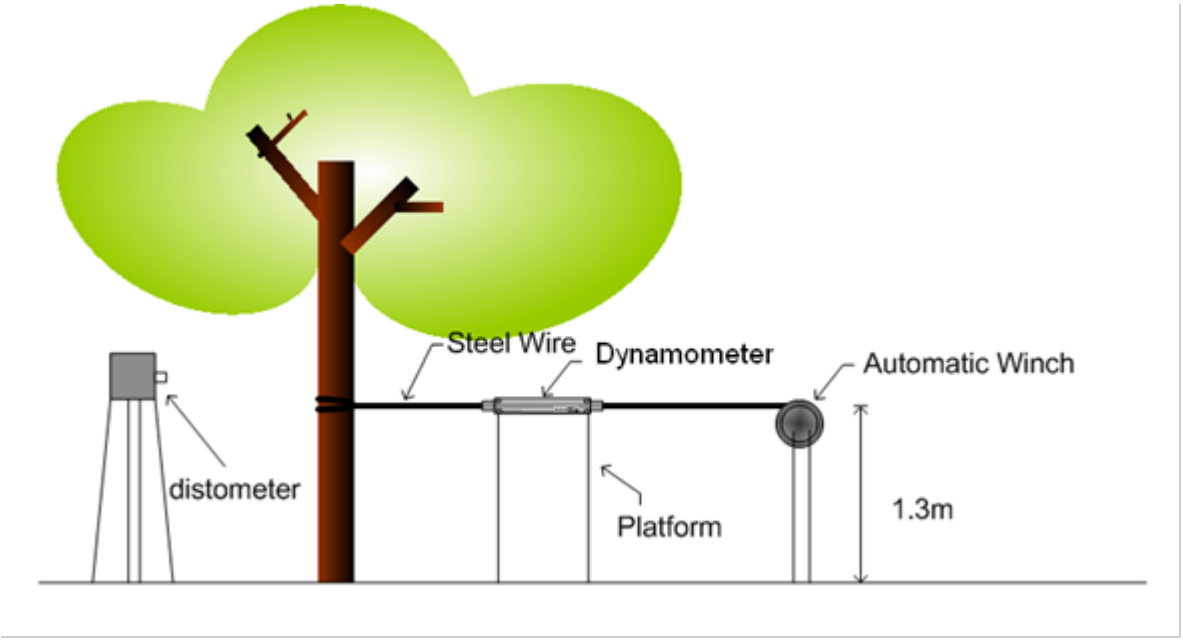

Figure 14 Tree pulling test set-up for tree pulling test (not to scale)

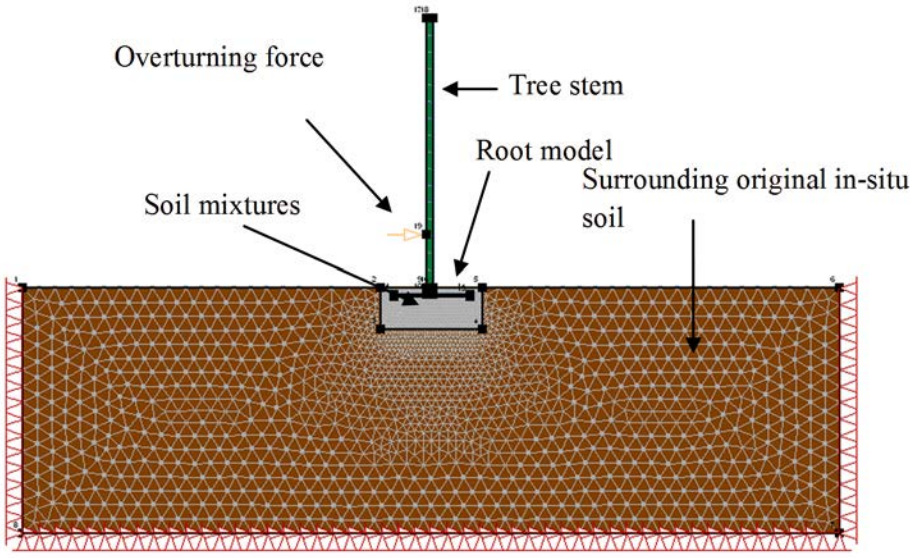

Figure 15 Numerical model of the pull out experiment

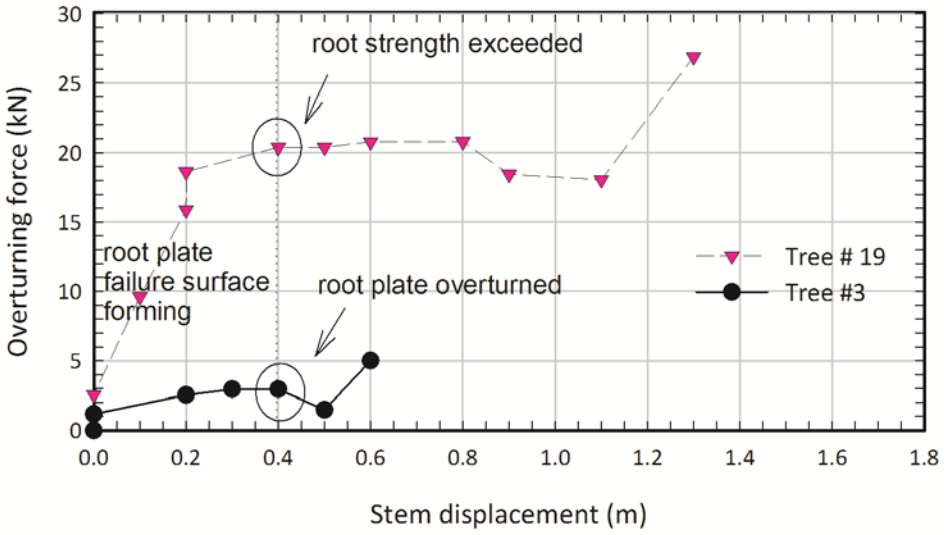

Figure 16 Typical force-displacement curve obtained from tree pulling test

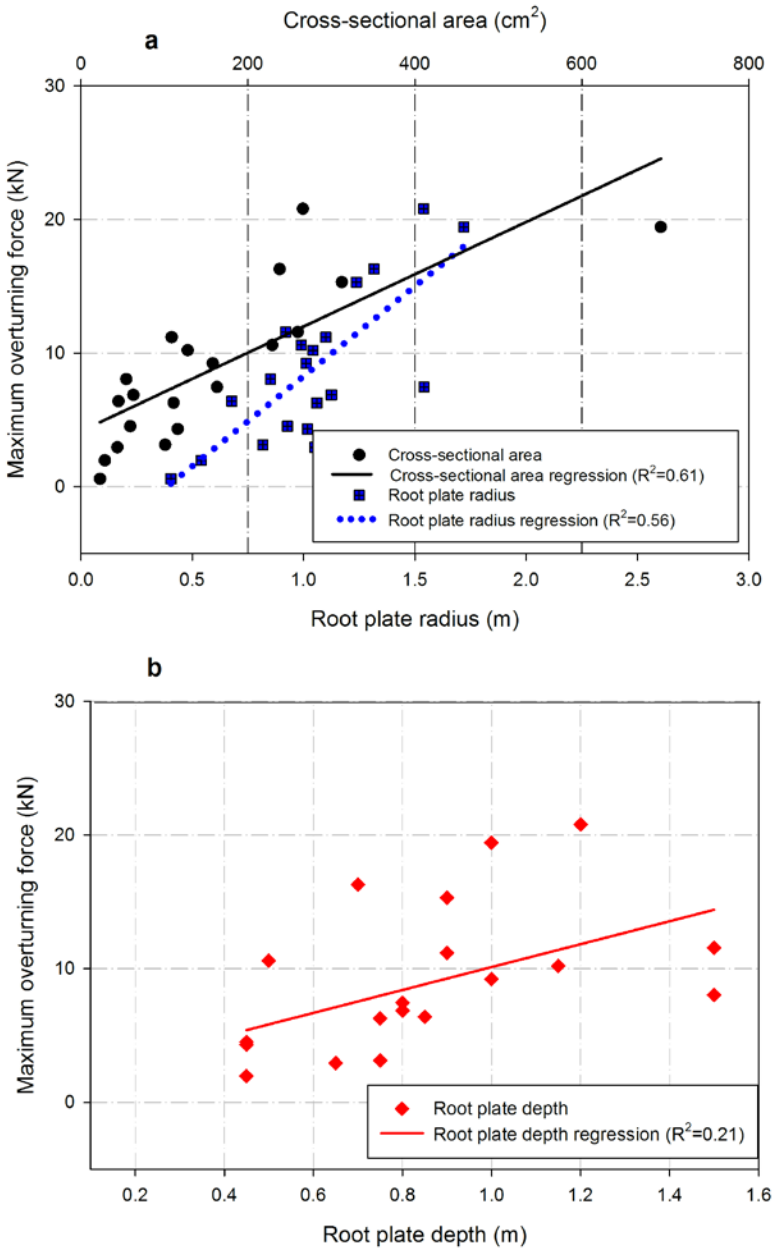

Figure 17 Correlations between maximum overturning force with a. root plate radius and cross-sectional area and b. root plate depth

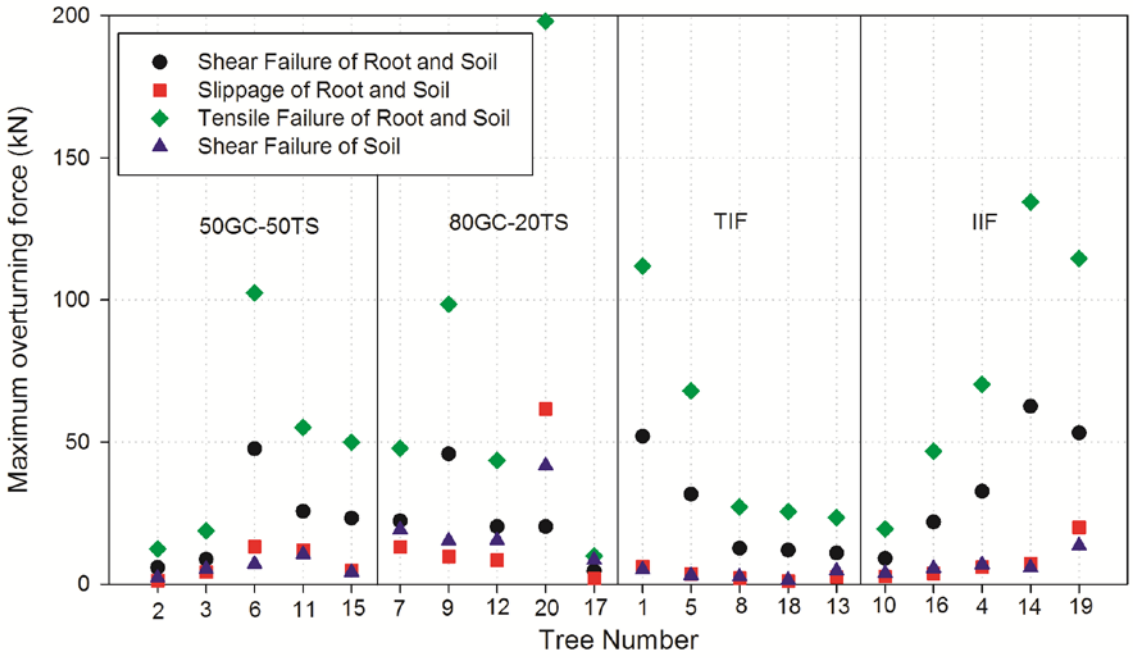

Figure 18 Analytical calculation results for different failure modes

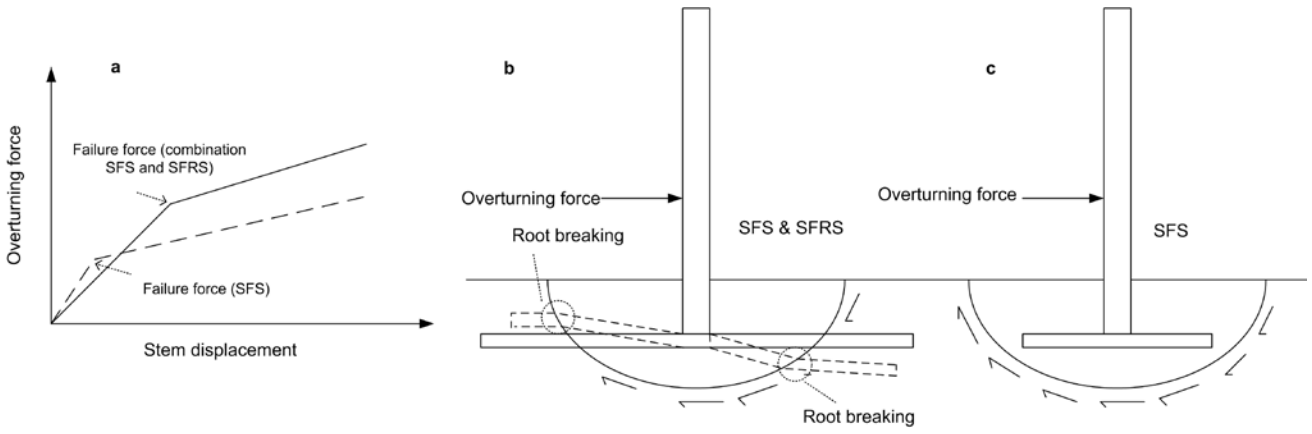

Figure 19 a. Typical force-displacement curve pattern obtained from numerical analyses.
b&c.Failure modes observed from numerical modeling

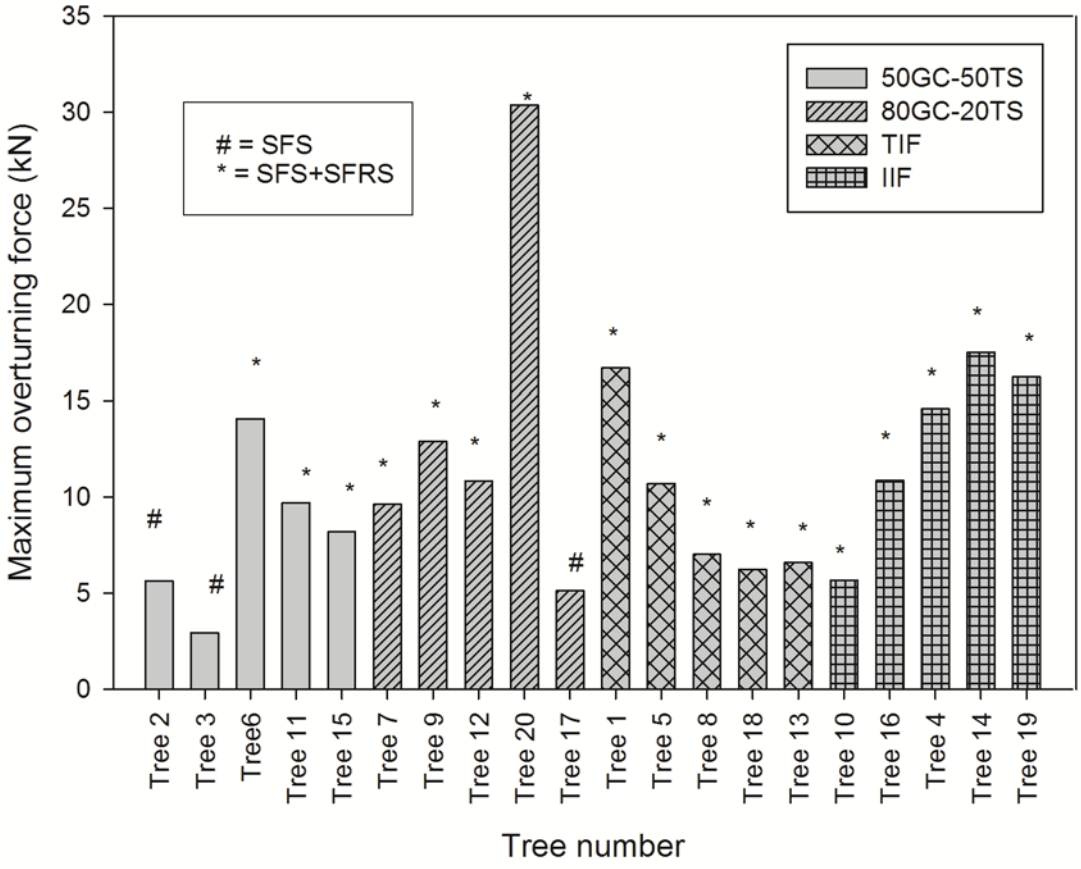

Figure 20 Maximum overturning force and failure mode obtained from numerical modeling

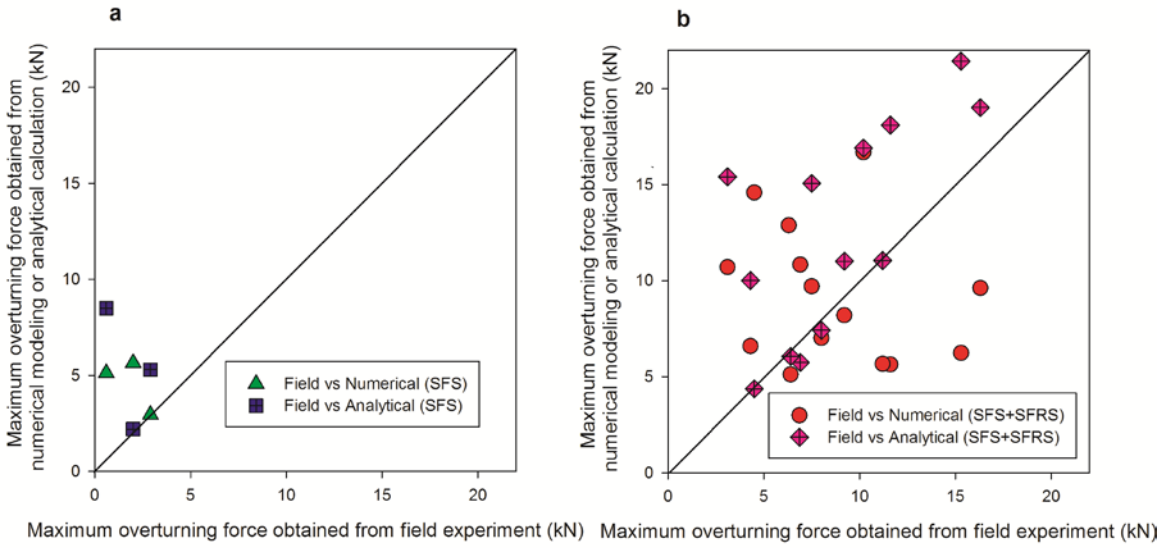

Figure 21 Comparison of overturning force obtained from tree pulling test and numerical modeling for a. SFS failure mode b. SFS+SFRS failure mode

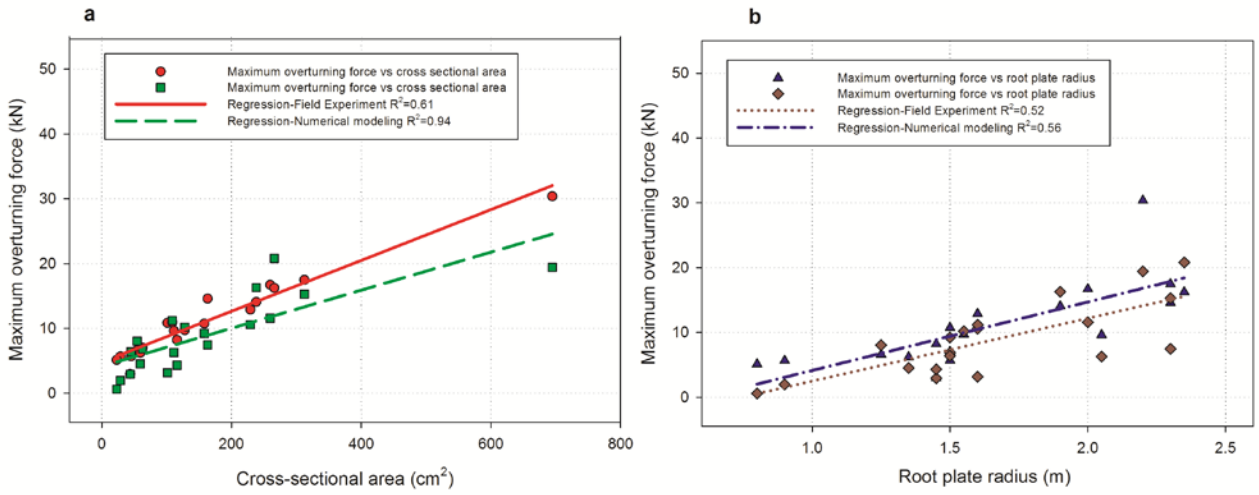

Figure 22 Relationship between the maximum overturning force and a. cross-sectional area, b root plate radius obtained from tree pulling test and numerical modeling

APPENDIX

Appendix 1 Tree characteristics recorded in the tree pulling test

Tree no	1	2	3	4	5	6	7	8	9	10
Soil type	TIF	50GC-50TS	50GC-50TS	IIF	TIF	50GC-50TS	80GC-20TS	TIF	80GC-20TS	IIF
CSA (cm^2)	259.9	28.8	43.7	163.2	158.2	238.2	111.2	62.9	229.2	45.2
Root depth (m)	1.5	0.5	0.7	0.8	1.0	0.7	0.8	0.8	0.5	0.9
radius of root plate (m)	0.9	0.5	1.1	1.5	1.0	1.3	1.1	1.1	1.0	0.7
Maximum Overturning force (kN)	11.6	2.0	2.9	7.5	9.2	16.3	6.3	6.9	10.6	6.4
Height (m)	6.6	6.6	6.6	6.6	6.6	7	6.8	6.5	6.5	6.5
Girth circumference (m)	0.55	0.4	0.4	0.55	0.58	0.63	0.54	0.45	0.53	0.42
Crown width (m)	9.5	2.8	5.2	5.8	7.8	7.88	7.05	3.2	4.6	5.3
Tree no	11	12	13	14	15	16	17	18	19	20
Soil type	50GC-50TS	80GC-20TS	TIF	IIF	50GC-50TS	IIF	80GC-20TS	TIF	IIF	80GC-20TS
CSA (cm^2)	128.07	101.23	54.47	312.53	116.16	108.93	23.09	59.32	266.06	694.64
root depth (m)	1.2	0.8	1.5	0.9	0.5	0.9	0.8	0.5	1.2	1.0
radius of root plate (m)	1.0	0.8	0.9	1.2	1.0	1.1	0.4	0.9	1.5	1.7
Maximum Overturning force (kN)	10.2	3.1	8.0	15.3	4.3	11.2	0.6	4.5	20.8	19.4
Height (m)	6.7	6.7	6.7	6.7	6.1	6.1	6.1	6.1	7	7
Girth circumference(m)	0.68	0.63	0.45	0.39	0.42	0.49	0.59	0.48	0.44	0.5
Crown width (m)	10.8	7.3	4.2	5.6	7.35	6.3	5.78	5.8	4.85	7.6